The unique ecological role of pyrosomes in the Eastern Tropical Pacific

Moira Décima [ORCID],[1]* **Michael R. Stukel** [ORCID],[2] **Lucía López-López**,[3,4] **Michael R. Landry**[5]

[1]National Institute of Water and Atmospheric Research, Wellington, New Zealand
[2]Department of Earth, Ocean, and Atmospheric Science, Florida State University, Tallahassee, Florida
[3]Imperial College London, United Kingdom
[4]Scripps Institution of Oceanography, Santander, Spain
[5]Scripps, Institution of Oceanography, University of California San Diego, La Jolla, California

Abstract

Pyrosomes are an important but often overlooked component of marine zooplankton communities, with limited existing information regarding their ecological and trophic roles in pelagic ecosystems. We present the first estimates of grazing and trophic interactions of the large tropical pyrosome, *Pyrostremma spinosum*, in the Eastern Tropical Pacific. While patchy in distribution, *Pyrostremma spinosum's* grazing impact was substantial, up to 17.5% of chlorophyll *a* standing stock d^{-1} in certain areas. In contrast, these organisms cleared a very small percentage of the abundant picoplankton *Synechococcus* spp. compared to the bulk zooplankton community. Stable isotopes (^{13}C and ^{15}N) indicated that particulate organic matter (POM) from the surface mixed layer (0–20 m) constitutes the isotopic food-web baseline for most of the zooplankton community, and zooplankton trophic interactions were size structured in some areas. Pyrosomes, doliolids, and appendicularians, along with the smallest size class of net-collected zooplankton, had isotopic values closest to pure herbivory, while intermediate size classes, copepods, and salps showed substantial omnivory/carnivory. Euphausiids, chaetognaths, and > 2 mm zooplankton were the main carnivorous zooplankton in the plankton food web. Stable isotopes indicated that *Pyrostremma spinosum* is trophically distinct from the rest of the zooplankton community, grazing just below the mixed layer (20–40 m), as opposed to feeding on surface POM. Pyrosomes represent an additional, distinct pathway for material transfer up the plankton food web, by directly consuming POM sources not substantially grazed upon by the rest of the mesozooplankton community.

Pyrosomes, the largest pelagic colonial tunicates, occur in most marine ecosystems from the warm tropics to cold temperate regions, yet their roles in marine food webs remain poorly known. From studies of pelagic tunicates (mainly of salps, doliolids, and appendicularians), we know that these organisms have general capabilities and functions that differ appreciably from their crustacean zooplankton counterparts (Alldredge and Madin 1982; Michaels and Silver 1988; Bone 1998). Their characteristics include gelatinous bodies, very high rates of reproduction, and the ability to form massive blooms (Andersen 1998; Deibel 1998; Fenaux et al. 1998). While feeding mechanisms of each group differ, their filtering modes are more efficient and allow much higher per capita

clearance rates than crustacean zooplankton (Bone 1998; Deibel 1998; Scheinberg et al. 2005; Hereu et al. 2010). In addition, the small pore sizes of their mucus filters allow capture of particles in the micron to submicron particle range, enabling the capture of bacteria and picophytoplankton not generally accessible to crustacean zooplankton (Madin and Kremer 1995; Zubkov and Lopez-Urrutia 2003; Scheinberg and Landry 2005; Sutherland et al. 2010). The combination of high particle consumption and growth rates of pelagic tunicates can also lead to substantial contributions to vertical export fluxes. When present in significant numbers, salps can dominate export due to high grazing and production of large fecal pellets that sink rapidly from the surface ocean with minimal microbial degradation (Madin 1982; Michaels and Silver 1988; Madin et al. 2006; Henschke et al. 2016; Stone and Steinberg 2016). The discarded mucus houses of appendicularians typically contain abundant fresh particles and can act as aggregation nuclei, attaching smaller particles as they contribute to the rain of marine snow (Alldredge 1972; Gorsky and Fenaux 1998; Lombard and Kiørboe 2010). Blooms of doliolids and salps further contribute to export by transporting carbon

*Correspondence: moira.decima@niwa.co.nz

to depth in sinking carcasses (Deibel 1998; Smith et al. 2014; Takahashi et al. 2015).

As the least studied pelagic tunicates, the pyrosome knowledge gap has been highlighted by recent observations of anomalously high pyrosome densities around the world, including the first observation of *Pyrosoma atlanticum* in the Canary Islands (Tobena and Escanez 2013), Taiwan (Kuo et al. 2015) and record densities in the California Current (Sakuma et al. 2016; Brodeur et al. 2018). The abundant and cosmopolitan species, *P. atlanticum,* is uniquely characterized by a tough, hard tunic resilient to net collections, colonies reaching sizes up to 17 cm (Van Soest 1981), and by swarms capable of removing substantial amounts of the phytoplankton standing stock (Drits et al. 1992; Perissinotto et al. 2007). To our knowledge, only one study has evaluated rates of fecal pellet sinking and degradation, suggesting sinking speeds (70 m d^{-1}) significantly less than those for salp pellets (Drits et al. 1992). While many studies support the idea that salps and appendicularians can tap into the microbial loop (Sutherland et al. 2010), comparable data on pyrosomes do not exist. Perissinotto et al. (2007) found higher retention efficiencies for cells greater than 10 μm in *P. atlanticum*, and fatty acids indicated a mixed phytoplankton diet of diatoms, dinoflagellates, and prymnesiophytes. *P. atlanticum* carcasses also contribute to carbon export, which can be substantial following blooms (Lebrato and Jones 2009; Liao et al. 2013).

We encountered large colonies of a pyrosome in the Eastern Tropical Pacific (ETP), later identified as *Pyrostremma spinosum*, a much lesser studied pyrosome with a more delicate consistency that *P. atlanticum*, as part of the Costa Rica Dome (CRD) FLUx and Zinc Experiments (FLUZiE) voyage (Landry et al. 2016*a*). The CRD is a unique open-ocean upwelling system within the ETP, characterized by very high abundances of *Synechococcus* spp., often exceeding 10^6 cells mL^{-1} (Li et al. 1983; Fiedler 2002; Selph et al. 2016), large zooplankton stocks (Décima et al. 2016), and a food web that supports many charismatic megafauna (including sea turtles, which feed on gelatinous zooplankton such as salps and pyrosomes) and top predators (Ballance et al. 2006). *Pyrostremma spinosum* has not, to our knowledge, been reported previously in the area (Van Soest 1981, 1998), but is known in other regions of the tropical Pacific (Griffin and Yaldwyn 1970; Van Soest 1998) as well as in the Arabian Sea (Gauns et al. 2015). We initially hypothesized that pelagic tunicates (anticipating mainly salps and appendicularians) would be uniquely equipped to capitalize on the large concentrations of picophytoplankton in the area. The occurrence of numerous large *Pyrostremma spinosum* colonies, however, provided an unexpected opportunity to investigate their roles in the trophodynamics and biogeochemistry of the area. In this study, we compare the grazing impacts of pyrosomes and size-fractionated mesozooplankton on phytoplankton and *Synechococcus* spp. using tracer pigments. We additionally investigate the resources sustaining zooplankton, using δ^{13}C and δ^{15}N of particulate organic matter (POM) to identify the vertical distributions of particles consumed by size-fractionated zooplankton, appendicularians,

salps, chaetognaths, ostracods, and pyrosomes, to construct a size-based assessment of material flows through the planktonic community, and to identify the likely source depth of particles sinking below the euphotic zone.

Material and methods

The FLUZiE voyage was conducted on the R/V *Melville*, from 22 June 2010 to 25 July 2010, in the area of 7.5–10.2°N, 87–93°W, in the ETP (Fig. 1). The sampling plan was based around semi-Lagrangian experiments, with each "cycle" of activity following a water parcel marked by satellite-tracked drogued drifters for 4–5 d (Landry et al. 2016*a*). We first conducted a transect across a broad area with elevated surface chlorophyll *a* (Chl *a*), to determine the center of the dome. The first cycle of the cruise was conducted in coastal waters and is not presented here. Cycle 2 was carried out in the central core area of the CRD, and Cycle 4 was initiated at the location of a drifter left to mark the movement of the same water where Cycle 2 ended 5 d earlier. Cycles 3 and 5 were located at the periphery of the dome, to the east and west, respectively (Fig. 1).

One drift array was used as a platform for in situ rate measurements including primary production (PP), phytoplankton growth, microzooplankton grazing, and nitrate uptake (Landry et al. 2016*a*). A second drift array had sediment traps at 90 and 150 m (Stukel et al. 2013). Net tows for zooplankton biomass and grazing estimates were conducted twice daily in the marked water parcels (Décima et al. 2016). Full descriptions of the experimental design, and references to studies already published from this cruise, can be found elsewhere (Landry et al. 2016*a,b*). Below, we provide details of the measurements that relate specifically to the current analysis.

Zooplankton sample collection

Mesozooplankton (> 200 μm) were collected with double-oblique tows taken twice daily from ~ 150 m to the surface between 10:00–13:00 h (daytime) and 21:00–24:00 h (nighttime) using a 1-m ring net fitted with a 202-μm Nitex mesh net, a temperature-depth logger, and a General Oceanics flow meter. Samples for biomass and gut-fluorescence grazing analyses were size fractionated (SF) using nested sieves into five size classes: 0.2–0.5, 0.5–1, 1–2, 2–5, and > 5 mm (Décima et al. 2016). Additional tows to 150 m, typically in late afternoon and at dusk, were conducted to collect live animals for experiments with other zooplankton (not presented here). *Pyrostremma spinosum* was mostly caught at night, with no specimens collected in morning or mid-day tows, strongly suggesting that the colonies were undergoing diel vertical migration (DVM), consistent with other species in the group (Andersen et al. 1992; Andersen and Sardou 1994; Bone 1998). Because the pyrosome colonies were relatively sparse but had a much greater biovolume when captured than the combined taxa of the regular net tows, we used catches from both standard night tows and evening live tows to estimate their
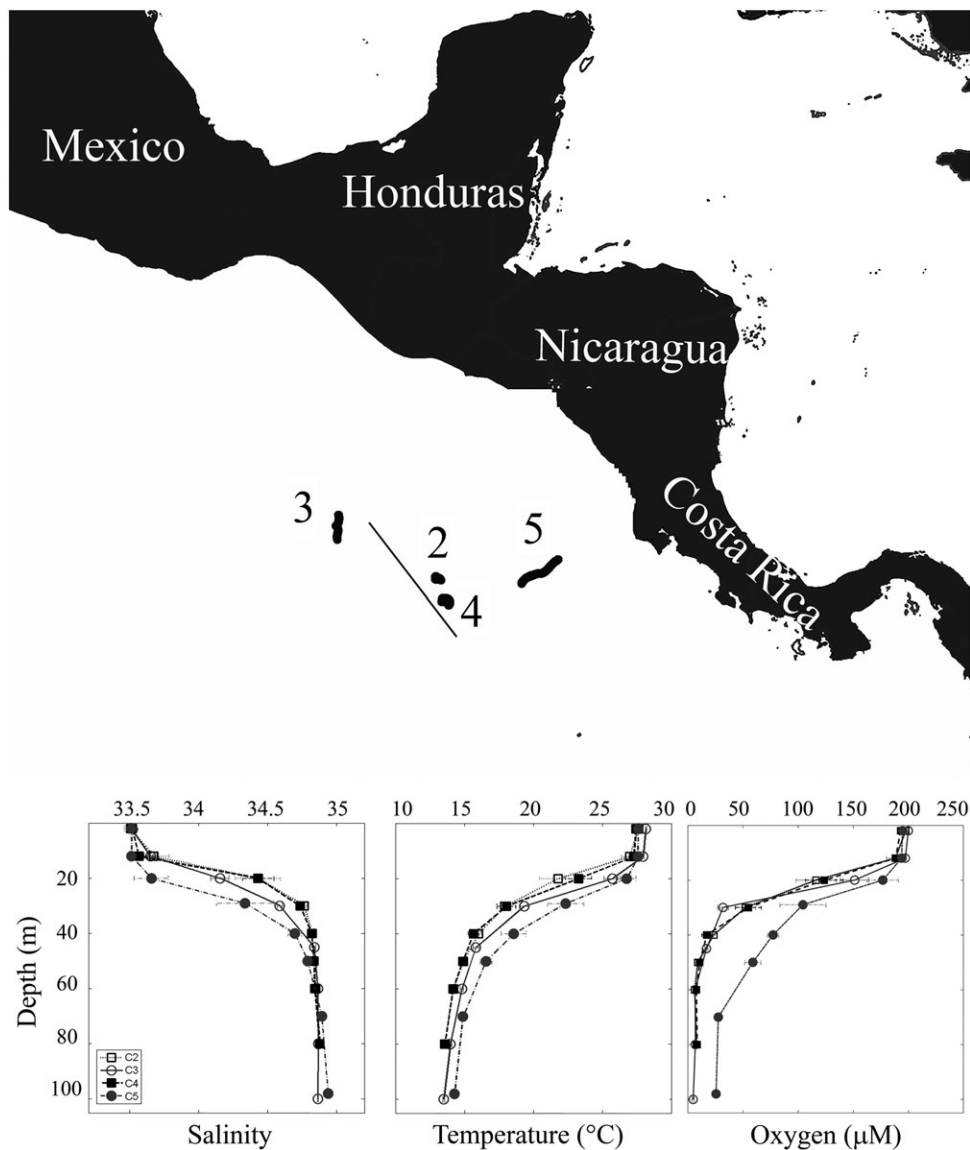
Fig. 1. Top panel shows experimental area, with numbers indicating cycle location. Lower panels indicate cycle mean depth profiles ($\pm$ SE) of salinity, temperature, and oxygen concentrations.

abundances and grazing impacts. These were combined by averaging the night catches (live and standard) only, not including day tows because of DVM.

Pyrostremma spinosum has a soft consistency and a tendency to break up in the nets. It should be noted that some literature citations refer to *Pyrosoma spinosum* (e.g., Griffin and Yaldwyn 1970; Gauns et al. 2015), but we use the cladistic classification from Van Soest (1998), which identifies this organism as *Pyrostremma spinosum*. However, the possibility of a new species cannot be discounted.

Our initial sampling plans were not optimized for capturing *Pyrostremma spinosum* (colonies were typically larger than the cod ends of our nets or the nested sieves used for size-fractionation). When it became apparent on Cycles 2 and 3 that

they were quantitatively important, we modified our methods to allow quantitative grazing and biogeochemical measurements of *Pyrostremma spinosum* on Cycles 4 and 5. We estimated size by measuring displacement volume and used this metric to extract standing stock and grazing estimates from the measurements made on pooled zooids. Collected pyrosomes, their displacement volumes, and analyzed specimens are indicated in Table 1. Subsamples of *Pyrostremma spinosum* were frozen at -80°C for later laboratory analysis.

Zooplankton grazing

Grazing rates for *Pyrostremma spinosum* were estimated by taking 2.5 mL aliquots (4 aliquots per specimen) of thawed pyrosome (9 ± 2 zooids), extracted in 10 mL of acetone

Table 1. Displacement volumes of *Pyrostremma spinosum* caught during FLUZiE zooplankton tows, estimated zooids per colony, and mean abundance per cycle.

Cycle	Days	Colony volume (liter)	Abundance (mL m^{-2} cycle^{-1})	Zooids per colony
Transect	Sta. 4	2.1	821.35*	7319 ± 138
2	5	0.5	10.56	1764 ± 106
3	2	0.03	9.74	106 ± 6
4	4	1.2[†,‡]	277.31	4233 ± 254
	5	2.0[†,‡]		7055 ± 423
	5	5.5[†]		19,400 ± 1162
5	2	3.7[†,‡]	118.13	13,051 ± 782
	4	0.6[†]		2116 ± 127

*Note that for Sta. 4 on the transect, the abundance was normalized by the one station, and is equivalent to abundance of one tow. Errors for zooid estimate per colony are SE.
[†]Organisms assayed for bulk isotopes.
[‡]Colonies assayed for gut pigments.

(90%), and sonicated with an ultrasonic tissue homogenizer. Samples were then allowed to extract for 2–4 h at −20°C, centrifuged for 5 min at 3000 × *g* to remove pyrosome tissue, and poured into 7-mL borosilicate tubes for fluorometric analysis. Pigments (Chl *a* and phaeopigments) were analyzed using a Turner 10AU fluorometer with a Chl *a* filter set, before and after acidification with two drops of 10% HCl (Strickland and Parsons 1972). A similar procedure was employed to measure phycoerythrin (PE), a pigment indicative of *Synechococcus* spp., using the glycerol uncoupling method. Aliquots for PE were transferred to a glycerol saline solution (50%), ground with a non-ultrasonic tissue homogenizer to release gut contents, and centrifuged to remove consumer tissues. Samples were measured on a Turner Designs TD-700 fluorometer with a PE filter set (Wyman 1992; Dore et al. 2002; Stukel et al. 2013). For each pyrosome, we calculated grazing as:

$$G = (pig \times f \times D \times 12 \times GCR)/vol$$

where *G* is grazing (mg m^{-2} d^{-1}), *pig* is the pigment gut (Chl *a* and phaeopigment or PE) content (mg), *f* is fraction of sample analyzed (2.5 mL/pyrosome volume), *D* is depth of tow (m), *vol* is volume of water filtered (m^3), and *GCR* is the gut clearance rate (h^{-1}). There is no GCR literature value for *Pyrostremma spinosum*, so we used the value of 0.699 h^{-1}, derived for *P. atlanticum* in the Indian Ocean at 13–15°C, which is similar to our temperatures below the thermocline (Perissinotto et al. 2007). Finally, we multiplied these estimates by 12 (h d^{-1}), consistent with the DVM observations noted above (Andersen and Sardou 1994; Bone 1998).

Detailed methods for estimates of size-fractioned mesozooplankton community grazing rates have been published elsewhere (Stukel et al. 2013; Décima et al. 2016). Briefly, we

used a method similar to that detailed above on the size-fractioned mixed community, using phaeopigment concentrations as the gut fluorescence estimate of herbivorous feeding to ensure that chlorophyll-containing phytoplankton aggregates caught by the net did not bias the grazing estimate. PE estimates of grazing rates on *Synechococcus* by the full zooplankton community were done similarly to those for *Pyrostremma spinosum*. The GCR for zooplankton was 2.1 h^{-1}, based on experimentally determined gut turnover rates in the Equatorial Pacific at similar mixed-layer (ML) temperatures (~ 25–27°C) (Zhang et al. 1995). For mesozooplankton, we multiplied day and nighttime rate estimates by 12 h each, and added the two for a daily grazing total.

Grazing impacts on the entire phytoplankton (Chl *a*) and *Synechococcus* (PE) communities were calculated by taking the daily averages of pigments consumed by each zooplankton group, normalized by the integrated pigment standing stock and multiplied by 100. Carbon egestion by zooplankton was estimated by multiplying the pigment-based rates times the C : Chl ratios from Taylor et al. (2016) at the appropriate feeding depths (see Data Analysis section below), and assuming an absorption efficiency of 0.7 (Conover 1966). We calculated mean regional grazing estimates for *Pyrostremma spinosum* by applying our rate determinations (e.g., mg Chl *a* eq. zooid^{-1} d^{-1}) from specific stations to the *pyrosome* abundances calculated for each cycle/station during the cruise, normalized by the sampling time (transect + Cycles 2–5), which was 23 d.

δ^{13}C and δ^{15}N determination

Eight depths from two casts with the conductivity-temperature-depth (CTD) rosette per cycle were sampled for water-column particulate organic carbon and nitrogen (POC, PON) and stable isotopes (^{13}C, ^{15}N). Samples were filtered onto pre-combusted glass fiber filters (GF/F) filters and frozen in liquid N$_2$, subsequently acidified, and analyzed by mass spectrometry. Samples from the shallow (90 m) sediment traps were prepared and analyzed in a similar manner (Stukel et al. 2016). Stable isotopes of size-fractionated zooplankton samples were measured on one day and one night tow, per cycle. Frozen samples were dried at 60°C for 24 h, and subsequently homogenized with a motorized tissue grinder in a glass test tube. Representative aliquots of each size (0.2, 0.5, 1, and 2 mm) were packed into individual tin cups for analysis. Stable isotopes of individual taxa were measured in two ways. Individuals from four groups (appendicularians, ostracods, calanoid copepods, and chaetognaths) were sorted from frozen samples, pooled and placed in tin cups, dried at 60°C for 24 h, packed, and analyzed for ^{13}C and ^{15}N. Individuals from fixed (formalin) samples were used for abundance estimates (published in Décima et al. 2016) and ^{15}N measurements but not C as the δ^{13}C increases in formalin preserved samples over time (Rau et al. 2003). Formalin preserved samples were subsampled to obtain specimens for: appendicularians, ostracods, doliolids, and euphausiids. Subsampling was done with a

Folsom splitter to obtain at least 100 individuals. Samples were sorted under a stereomicroscope, rinsed, imaged, and measured using Image J. Only euphausiids were identified to species (*Euphausia distinguenda*, *Euphausia lamelligera*, and *Euphausia eximia*). Average sizes were calculated for each group from the mean sizes in each cycle. Mean sizes for the size-fractioned community were taken as the midpoint of the size interval (i.e., 0.375, 0.75, 1.5, and 3.5 mm).

Bulk isotopes for salps were obtained for both the main body and the gut separately from frozen samples. Using a thin blade scalpel, the guts of individual salps were excised, put into tin cups and dried for later analysis. The remaining body was processed in the same manner. For *Pyrostremma spinosum*, portions of approximately 40–60 zooids per colony were excised, dried at 60°C for 24 h, packed in tin cups and analyzed.

All isotope determinations were conducted at the Isotope Biogeochemistry lab at Scripps Institution of Oceanography. Isotope samples were neither acidified or lipid extracted prior to analyses. Acidification was not done because there were relatively few carbonate-containing organisms in our zooplankton tows (Décima et al. 2016), and acidification has been shown to artificially decrease both δ^{13}C and δ^{15}N values (Ute et al. 2005). ^{13}C values of thinly calcified ostracods could be slightly enhanced due to this decision (which we address in the discussion), but those values were within the measured range for the rest of the community (Supporting Information Fig. S1). Additionally, ostracods, while never dominant, were most abundant for Cycle 3 (Décima et al. 2016), but size-fractioned δ^{13}C values for that cycle were within the same range as the others (Supporting Information Fig. S1). Lipids are typically significantly depleted in δ^{13}C, and large amounts, as occurs in fish, mammals, and many polar zooplankton, can significantly bias their carbon isotopic values (Logan et al. 2008). However, the zooplankton of tropical regions like the CRD generally do not accumulate lipid stores (Lee et al. 2006), and pelagic tunicates and gelatinous organisms, in particular, have negligible lipid accumulation (Madin et al. 1981; Deibel et al. 1992; Nelson et al. 2000). Ricca et al. (2007) advise against lipid extraction for lower pelagic food-web members, especially if nitrogen is of particular interest, and high precision of δ^{13}C is not required. Mintenbeck et al. (2008) have also shown that lipid extraction can alter δ^{15}N values significantly, up to 1.65‰.

Data analysis

The feeding depths of individual zooplankton groups were evaluated relative to POM isotope profiles. These were separated into four depth strata: 0–20, 21–40, 41–60, and 61–100 m, the deeper depths of each strata roughly corresponding to: the ML, 20°C isotherm, euphotic zone, and sub-euphotic zone, although these were quite variable among cycles (Taylor et al. 2016). Trophic discrimination factors (TDF; Δ) were added to water-column POM values for both δ^{13}C and δ^{15}N. Because fractionation can vary among species, we drew consumer polygons that included the POM

measurement (Δ^{13}C = Δ^{15}N = 0), and the POM measurement plus Δ^{13}C = 0.5‰ and Δ^{15}N = 2.5‰. These numbers are consistent with TDF literature values (Vander Zanden and Rasmussen 2001; Post 2002; Williams et al. 2014), although slightly lower than the typical 3.4‰, as we chose the Δ^{15}N to ensure no animal had a trophic position (TP) < 2 (see below). These consumer polygons delimit the isotope area in which particle feeders should fall, encompassing all the possible isotopic values that a particle grazer could have if consuming locally available POM nonselectively.

Zooplankton TPs were calculated using POM values as a baseline, as follows:

$$TP = \left(\delta^{15}N_{consumer} - \delta^{15}N_{POM}\right)/\Delta^{15}N + 1$$

where $\delta^{15}N_{consumer}$ corresponds to the zooplankton value, and $\delta^{15}N_{POM}$ is the POM value at the baseline depth, based on feeding depths determined using POM consumer polygons. We used 2.5 as a TDF to ensure that size-fractioned zooplankton had TP ≥ 2. This value is consistent with other studies of marine zooplankton trophic enrichment (e.g., Rau et al. 2003). We consider the problem of baseline variability on TP estimates in the discussion. TDFs for salps were assessed by comparing δ^{15}N tissue to δ^{15}N gut. Consumer polygons and other data analyses were made using Matlab 2013a.

Results

Oceanographic conditions

The ML depth at ~ 20–30 m was clearly identified by the abrupt decrease in temperature and dissolved oxygen concentrations, and increase in salinity values (Fig. 1), with particle and plankton concentrations closely tied to these water-column physical properties. Chl *a* peaked in the ML (Fig. 2a), suspended phaeopigment maxima were just below the ML (Fig. 2b), *Synechococcus* spp. concentrations peaked typically at the surface (Fig. 2c), with highest concentrations of 2×10^5 cells mL^{-1} in the dome center, and larger phytoplankton (> 2-μm cells) decreased from surface to depth (Fig. 2d). Particle concentrations were highest at the surface, decreasing somewhat monotonically from surface to roughly 60 m (Fig. 3a,b), yet PO^{13}C and PO^{15}N showed differing vertical profiles. δ^{13}C values were highest in particles in the upper 20 m (−21‰) and decreased rapidly to −26‰ at 40 m, changing little at deeper depths (Fig. 3c). Vertical profiles of PO^{15}N were enriched in ^{15}N in the upper 20 m and at depth (60–80 m), with local minima at intermediate depths (30–40 m), depleted by up to 4‰ compared to surface values (Fig. 3d). Surface δ^{15}N values ranged from 4‰ to 7‰, while deep PO^{15}N (70–80 m) was consistently ~ 7‰.

Pyrostremma spinosum abundance and grazing

Individual pyrosome colonies varied in biovolume from 25 mL to 5.5 L, resulting in total tow densities of
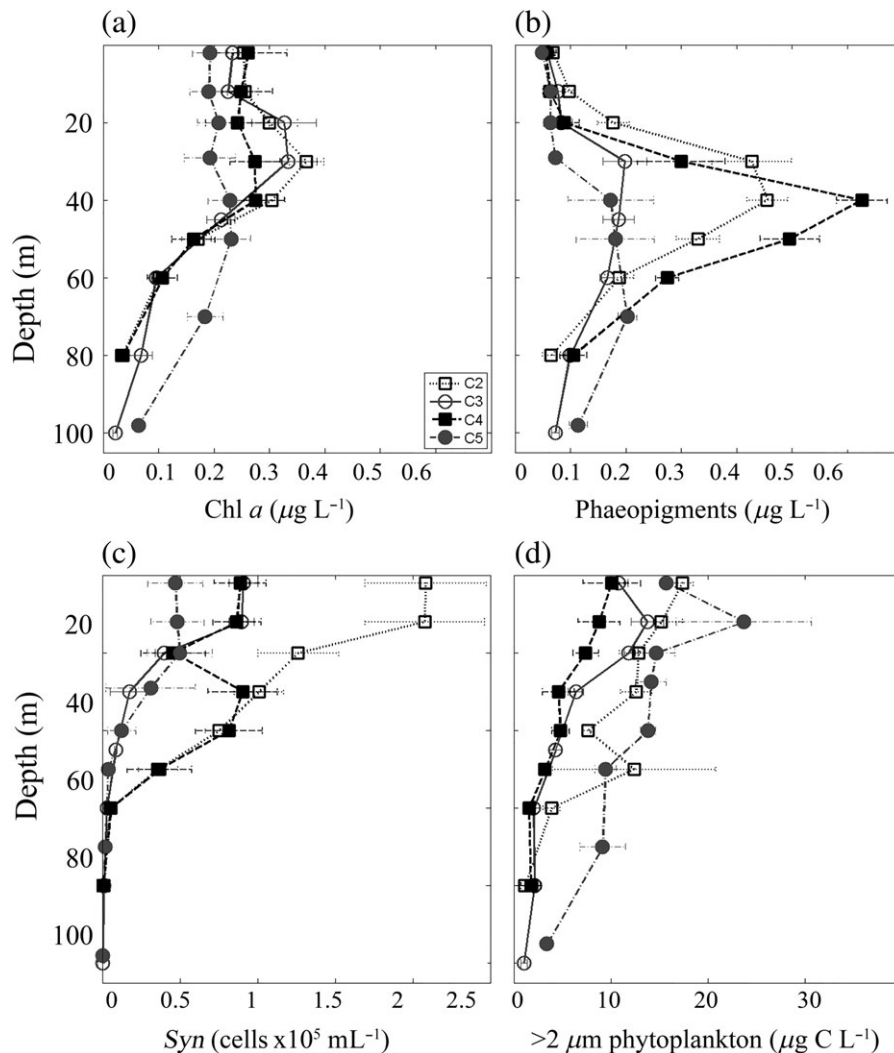
Fig. 2. Mean cycle vertical profiles of **(a)** Chl *a*, **(b)** phaeopigments, **(c)** *Synechococcus spp.* abundance, and **(d)** > 2-μm phytoplankton cell carbon. Error bars are SEs of five CTD casts taken daily at noon.

0.04–2.7 L m^{-2} (Table 1). Due to possible break up during net capture, the lower estimates may not represent full colonies. From visual observations, intact *Pyrostremma spinosum* floating near the sea surface at night were 0.5–2 m in length, consistent with net-collected animals during this part of the cruise (Table 1). Pyrosome grazing rates were very high due to large colony size, with up to 20,000 zooids colony^{-1} (Table 1), and high pigment content per zooid (Table 2). Regional grazing impacts of pyrosomes were variable, with a single colony capable of removing up to 36% of Chl *a* standing stock (Table 3). However, due to low abundance and patchy distribution, the integrated value over a single water patch varied between 0.7% and 17.5%, with an overall cruise mean of 4.2% ± 2.1% (Table 3). Compared to ingested Chl *a* + phaeo, PE concentrations (1–1.9 μg per zooid) were low in all analyses (Table 2), resulting in insignificant percentage removal of *Synechococcus* standing stock d^{-1} by pyrosome colonies (Table 3).

Trophic niches within the water column

The vertical distributions of PO^{13}C and PO^{15}N are useful for determining the sources of material for particle-feeders, as different strata were found to have different δ^{13}C and δ^{15}N values, with δ^{13}C of −24‰ to −23‰ found only in the layer immediately below the ML, and lowest δ^{15}N values present uniquely in subsurface waters as well (Fig. 3; Table 4). Consumer polygons delineating the isotope space for animals feeding in each of these depth strata were constructed using combined data from all locations. While the individual cycles showed almost no overlap between the two shallowest depth strata (Supporting Information Fig. S1), the regional averages had greater overlap between the surface (0–20 m) and the 21–40 m strata. The deeper strata (41–60 and 61–100 m) were always clearly separated from the shallow surface ML (Fig. 4).

δ^{13}C and δ^{15}N values for size-fractioned zooplankton, most of the zooplankton taxonomic groups, and pelagic tunicates
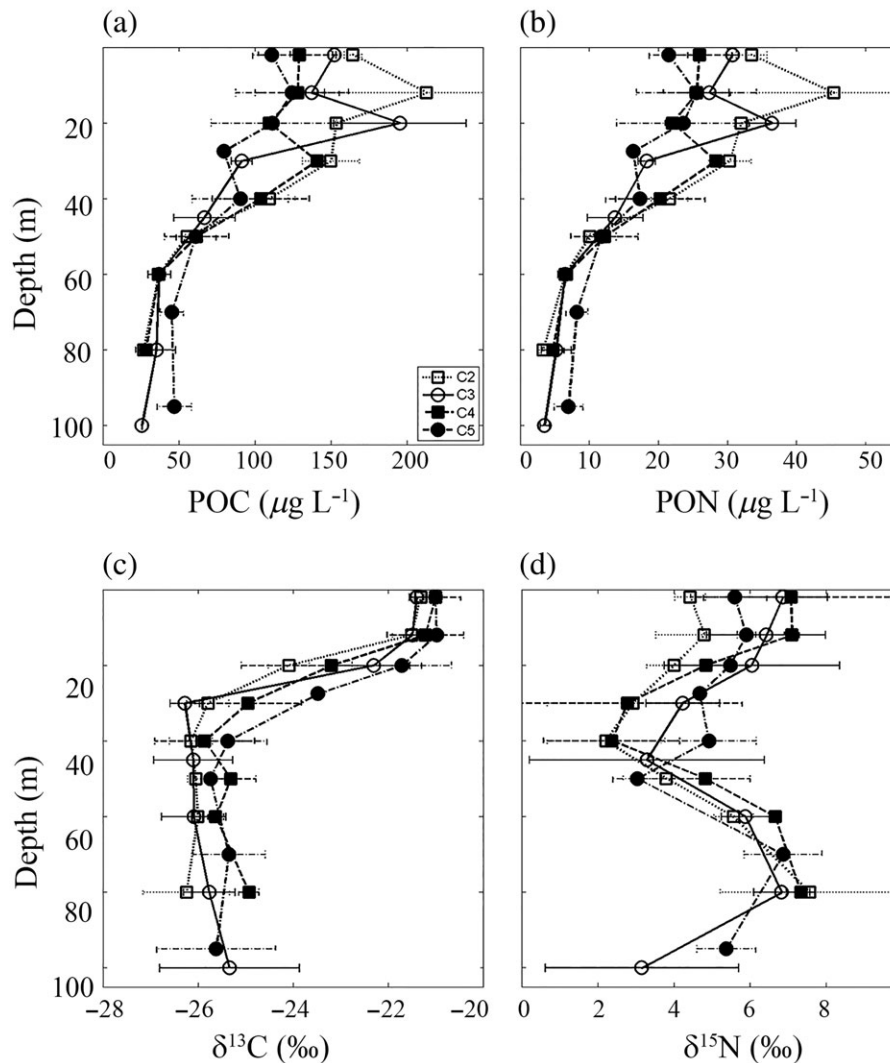
Fig. 3. Mean vertical profiles of **(a)** POC, **(b)** PON, **(c)** PO^{13}C, and **(d)** PO^{15}N. Error bars are standard deviation of two CTD casts per cycle (2–4).

Table 2. Average quantities for pigment per zooid: Chlorophyll *a* (Chl *a*), phaeopigments (Phaeo), phycoerithryn (PE), and phaeo : Chl *a*.

Cycle	Chl *a* Ng pigment per zooid	Phaeo Ng pigment per zooid	PE Ng pigment per zooid	Phaeo : Chl *a*
4	74 ± 61	362 ± 292	1.9 ± 0.4	4.9
5	56 ± 20	206 ± 89	1.0 ± 0.2	3.7

(with the exception of pyrosomes) fell within the 0–20 m depth polygon (or outside with slightly higher values). This suggests that surface production was fueling these assemblages, although most organisms (including salps) exhibited varying degrees of omnivory/carnivory, resulting in higher $\delta^{13}C$ and $\delta^{15}N$ isotope values (Fig. 4 and Supporting

Information Fig. S1; Table 4). Sediment trap values, in contrast, suggested that material sinking across the 90-m depth horizon originated from the euphotic zone below the ML, with lower values for both $\delta^{15}N$ and $\delta^{13}C$, despite high variability among replicates (Fig. 4). Most interestingly, bulk isotopes of *Pyrostremma spinosum* indicated that they were the only group consistently feeding at depths below 20 m, and had isotope values similar to sediment trap material from 90 m. On only one out of our four Lagrangian cycles, size-fractioned zooplankton displayed a range of $\delta^{13}C$ values, suggesting that larger organisms can feed on particles or organisms from deeper depths (Supporting Information Fig. S1; Fig. 4). Salps and appendicularians had similar isotopic contents to small zooplankton, ostracods, and copepods, all feeding on the POM baseline originating at the surface. Chaetognaths and > 1-mm zooplankton had the highest ^{15}N values, suggesting enhanced levels of carnivory (Fig. 4).

Table 3. Grazing impact of mesozooplankton (> 200 μm) and pyrosomes on Chl *a* and *Synechococcus* (Syn), expressed as percent removed per day. Mean ± Std of each cycle. Sta. 4 during the line transecting the dome represents one station where a large *Pyrostremma spinosum* was collected, and does not correspond to any of the cycles. Nd indicates no data.

Cycle	Chl *a* standing stock	Impact on Chl *a*	
		Mesozooplankton	Pyrosomes
	Mg Chl *a* m^{-2}	%	%
Sta. 4	25.3	6.3	36.2 ± 26.3*
2	17 ± 4.2	9.8 ± 3.4	3.2 ± 2.3*
3	17.2 ± 3.5	23.1 ± 9.84	0.7 ± 0.5*
4	14.9 ± 2.9	21.8 ± 10.4	17.5 ± 6.7
5	16.8 ± 4.8	44.6 ± 18.8	6.6 ± 2.4
FLUZiE average	19.2 ± 5.0	14.2 ± 10.6	4.2 ± 2.1

Cycle	Syn biomass Cells m^{-2}	Impact on *Synechococcus* spp.	
		Mesozooplankton %	Pyrosomes %
Sta. 4	1.0×10^{12}	Nd	0.6 ± 0.2*
2	7.1 ± 0.8×10^{12}	0.5 ± 0.2	0.02 ± 0.01*
3	2.0 ± 0.3×10^{12}	2.9 ± 0.8	0.02 ± 0.01*
4	3.3 ± 0.7×10^{12}	0.9 ± 0.6	0.05 ± 0.02
5	8.4 ± 2.5×10^{11}	5.1 ± 1.3	0.3 ± 0.3
FLUZiE average	3.0 ± 2.1×10^{12}	2.3 ± 2.1	0.04 ± 0.02

Indirect grazing estimates, based on gut pigment measurements normalized by pyrosome biovolume conducted in Cycles 4 and 5, and applied to the measured pyrosome abundances.

Omnivory of salps was supported by visual investigations of fecal pellets produced during incubations of freshly collected organisms. These showed a mixed diet including copepods, ostracods, radiolarians and phytodetritus (Fig. 5). We attempted to estimate TDFs from the isotopic differences between gut contents and bulk tissues of salps, but the results were quite variable, with salp tissues typically enriched by 0.1‰ to 2.1‰, relative to guts, for both ^{13}C and ^{15}N (Table 5).

TP with zooplankton size

Increasing TP with organism size was observed up to the 1–2 mm size class in the bulk zooplankton community, with these zooplankters having the highest TP of all groups (2.8 ± 0.1, mean ± SE) followed closely by chaetognaths, euphausiids, and > 2 mm zooplankton, with TP ~ 2.7 (Fig. 6). Herbivorous copepods (TP = 2.2 ± 0.2, mean ± SE) and ostracods (TP = 2.4 ± 0.1, mean ± SE) had slightly lower TPs than expected for their size, based on the pattern observed for the size-fractionated community. Pelagic tunicates did not follow size-structured patterns in TP like the bulk zooplankton community. Pyrosomes had the lowest TP (1.1 ± 0.1, mean ± SE), followed by doliolids (1.3 ± 0.1, mean ± SE) and appendicularians

Table 4. Percent carbon, C:N (g:g), stable isotope composition of mesozooplankton, salps, and *Pyrostremma spinosum*. Mesozooplankton values are a biomass-weighted average of all size-classes. Nd indicates no data.

	%C	C : N	δ^{13}C	δ^{15}N
Cycle 2				
Mesozooplankton	37.6 ± 2.1	3.8 ± 0.2	−19.9 ± 0.1	9.4 ± 0.6
Salps	Nd	Nd	Nd	Nd
Pyrostremma spinosum	Nd	Nd	Nd	Nd
Sediment trap	—	9.6 ± 0.7	−24.1 ± 1.6	14.3 ± 9.1
Cycle 3				
Mesozooplankton	33.4 ± 6.2	3.9 ± 0.3	−20.4 ± 0.1	10.8 ± 1.4
Salps	16.5 ± 9.4	5.0 ± 0.4	−20.8 ± 0.3	8.4 ± 0.7
Pyrostremma spinosum	Nd	Nd	Nd	Nd
Sediment trap	—	11.7 ± 2.2	−24.4 ± 0.1	4.6 ± 3.6
Cycle 4				
Mesozooplankton	36.4 ± 1.0	3.6 ± 0.3	−20.4 ± 0.4	9.8 ± 0.4
Salps	Nd	Nd	Nd	Nd
Pyrostremma spinosum	10.2 ± 4.2	6.3 ± 1.0	−23.8 ± 1.0	4.5 ± 0.8
Sediment trap	—	10.9 ± 0.7	−24.0 ± 0.0	5.3 ± 1.7
Cycle 5				
Mesozooplankton	39.11 ± 0.04	4.0 ± 0.1	−22.3 ± 0.1	9.4 ± 0.3
Salps	13.3 ± 5.9	4.7 ± 0.8	−19.0 ± 0.7	9.7 ± 0.4
Pyrostremma spinosum	8.1 ± 0.9	6.3 ± 0.2	−23 ± 0.4	5.1 ± 0.5
Sediment trap	—	11 ± 1.76	−24.1 ± 0.2	6.9 ± 0.6

(1.8 ± 0.1, mean ± SE), and salps had the highest TPs (2.2 ± 0.1, mean ± SE) of the group (Fig. 6). Regional differences in trophic structure with size were present in our study, with organisms displaying higher absolute TPs in the center of the dome (TPs > 3 for large bulk and crustacean zooplankton), and somewhat lower TPs outside of the dome (Supporting Information Fig. S2).

Discussion

The pyrosome *Pyrostremma spinosum* appears to occupy a distinct vertical niche in the pelagic habitat of the ETP. Their isotopic values differ significantly from all the other groups in the zooplankton assemblage, matching the profile below the surface ML, and resembling the material exported to sediment traps. While they contribute little to the grazing impact on *Synechococcus* (the dominant phytoplankter, constituting 20–30% of autotrophic carbon), they have a high grazing impact on deeper dwelling phytoplankton, and likely the sinking aggregate pool, impacting export through the base of the euphotic zone. In the following discussion, we consider these ecological roles in comparison to other zooplankton taxa and the lower food-web dynamics and biogeochemistry of the region.

Trophic flows through zooplankton

Consumer polygons, TP estimates, and pigment-based grazing depict a zooplankton community largely fueled by surface
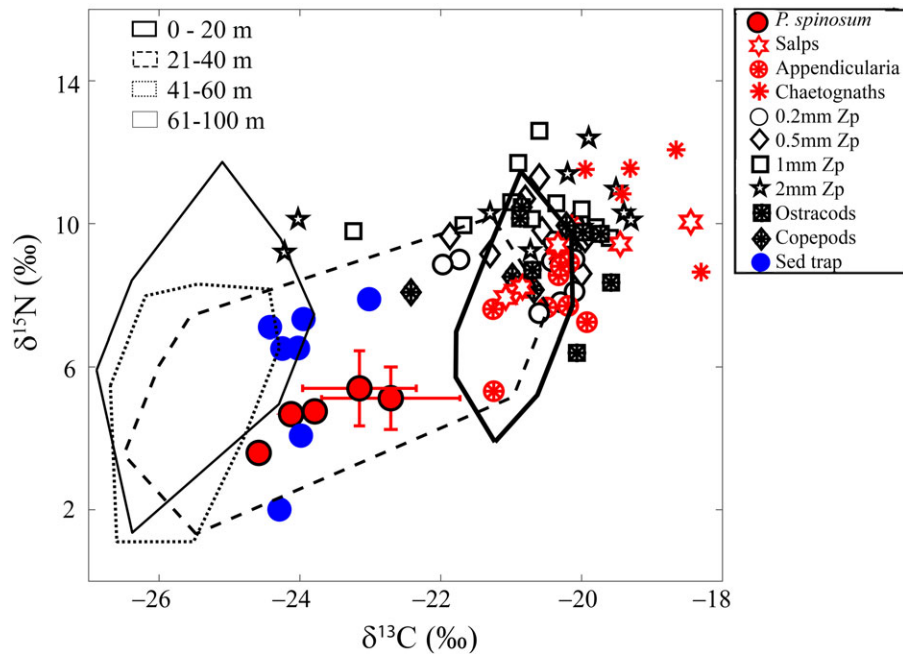
Fig. 4. Consumer polygons of vertically resolved POM. Thick solid line polygon represents 0-20 m, dashed line represents 21-40 m, dotted line 41-60 m, and thin solid line is 61-100 m POM. Black open symbols are different size fractions of zooplankton. Hatched symbols are broad zooplankton taxonomic groups. Symbols in red are gelatinous (*Pyrostremma spinosum*, salps, appendicularians, and chaetognaths) zooplankton, and blue indicates values from sediment traps.

production, with significant levels of carnivory and omnivory, and a separate pyrosome assemblage sustained by phytoplankton residing just below the ML. While inferences based on bulk isotopes can be complicated by isotopic variability of the POM baseline (Post 2002; Chouvelon et al. 2012; Décima et al. 2013), significant amounts of inorganic carbon (Ute et al. 2005), or substantial lipids in zooplankton samples (Ricca et al. 2007; Mintenbeck et al. 2008), these factors likely do not significantly affect our conclusions. POM-based polygons were constructed using eight measurements at each depth, over a large area (Fig. 1), carried out over a 20-d period, which likely decreased the effect of high-frequency variability on the baseline of each cycle (Fig. 4; Supporting Information Fig. S1). Zooplankton isotope values are consistent with low amounts of inorganic carbon and lipids, as ostracods did not have substantially higher $\delta^{13}C$ values than the rest of the zooplankton community, and bulk zooplankton were not significantly depleted in $\delta^{13}C$ (a consequence of high lipid concentrations; Fig. 4). If we were to apply a general mathematical correction (Post et al. 2007), our sample values would shift to the right, resulting in zooplankton with highly enriched $\delta^{13}C$ values well outside any of the consumer polygons. In addition, our results agree with other stable isotope determinations from the area (Williams et al. 2014), and our own visual observation of salp fecal pellets (Fig. 5) containing large copepods, ostracods, and radiolarians, along with phytodetritus.

The TP estimates for salps, reflecting substantial omnivory (mean = 2.24, range = 1.9–2.8, Fig. 6), are conservative if the TDF value that we used (2.5‰ for ^{15}N) is too high, as suggested by the body-gut difference from Table 5, from which we can calculate a mean TDF of 1‰ (range 0.1–1.9). If we use this empirically derived TDF for thaliaceans in general, our isotope measurements would give a mean TP = 2 (range 0.5–3.2) for doliolids, as opposed to the unrealistic estimates in Fig. 6. While we can also generally attribute the low TP estimates for *Pyrostremma spinosum* to uncertainties in the applicable TDF values for such consumers, one specimen had ^{15}N values less than the PO^{15}N of the intermediate depth stratum (less than any PO^{15}N sampled), indicating that it had grown under food conditions that differed in ^{15}N content from the water column where it was collected. This decoupling is not surprising given that *Pyrostremma spinosum* migrate to deeper depths with different currents during daytime.

We generally interpret the isotope enrichment of mesozooplankton as not accounting for the transfers through protistan microzooplankton, because prior studies have shown that phagotrophic protists increase only minimally in $\delta^{15}N$, up to 0.5‰, with trophic transfers (Gutiérrez-Rodríguez et al. 2014; Décima et al. 2017; Landry and Décima 2017). Other lines of evidence from experimental studies, however, have demonstrated the importance of microzooplankton as prey for openocean mesozooplankton generally (Stoecker and Capuzzo 1990; Fessenden and Cowles 1994; Roman and Gauzens 1997;
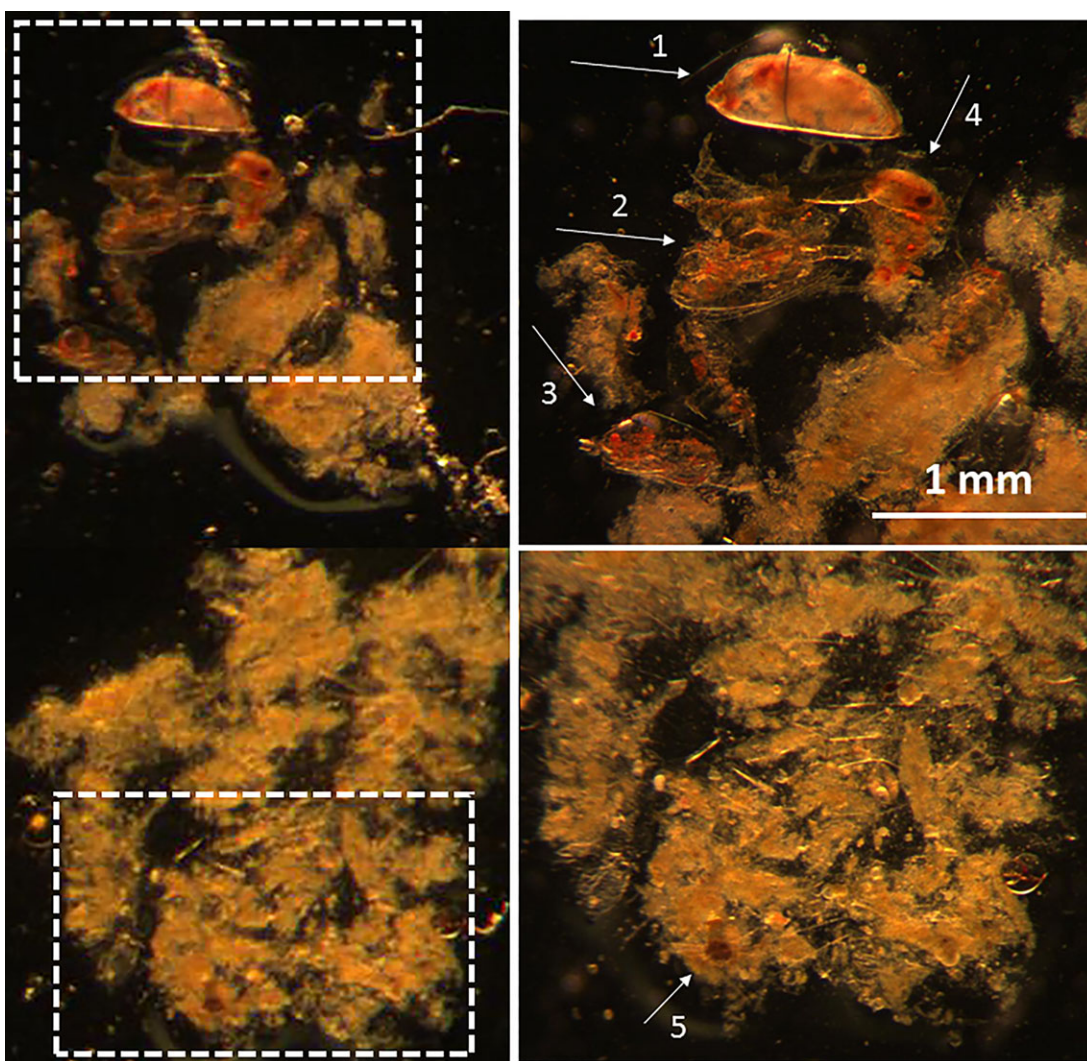
Fig. 5. Contents of two fecal pellets collected from healthy salps. Panels to the right are blow-ups of the areas indicated in dashed lines. Arrows indicate heterotrophic prey items. Arrows 1, 3, and 4 indicate ostracods, arrow 2 indicates a copepod, and arrow 5 points to a radiolarian, with phytodetritus surrounding these prey items.

Table 5. Salp body and salp gut bulk isotope values, collected during cycle 3 and cycle 5 in the CRD.

| Cycle | Salp form | Body | | | | Gut | | | | $\Delta^{15}N$ | $\Delta^{13}C$ |
		$\delta^{15}N$	$\delta^{13}C$	%C	C : N	$\delta^{15}N$	$\delta^{13}C$	%C	C : N		
3	Aggregate	9.4	−19.5	9.9	5.3	8.3	−20.0	15.3	5.4	1.1	0.5
3	Aggregate	10.0	−18.5	23.1	4.2	8.1	−20.6	16.4	6.1	1.9	2.1
5	Aggregate	8.1	−20.9	17.3	5.4	6.9	−21.5	28.1	5.3	1.2	0.5
5	Aggregate	7.9	−21.1	19.2	5.1	6.3	−21.1	24.2	6.6	1.6	0.1
5	Solitary	9.4	−20.3	10.2	4.6	9.3	−20.8	12.9	4.9	0.1	0.5
5	Solitary	8.2	−20.8	6.6	4.8	8.0	−21.9	8.2	5.4	0.3	1.0

Calbet and Landry 1999; Liu et al. 2005; Landry et al. 2016*b*; Décima et al. 2017), and as a major trophic pathway to meso-zooplankton in the ETP (Stukel et al. 2013; Stukel et al. 2016; Landry et al. 2016*b*). In fact, it would be possible for some of the deeper (20–40 m) material to support zooplankton production, but this would require an average TP ≥ 3 for phago-trophic protists (assuming a 0.5‰ isotopic enrichment), as intermediate prey, to be consumed by the mesozooplankton
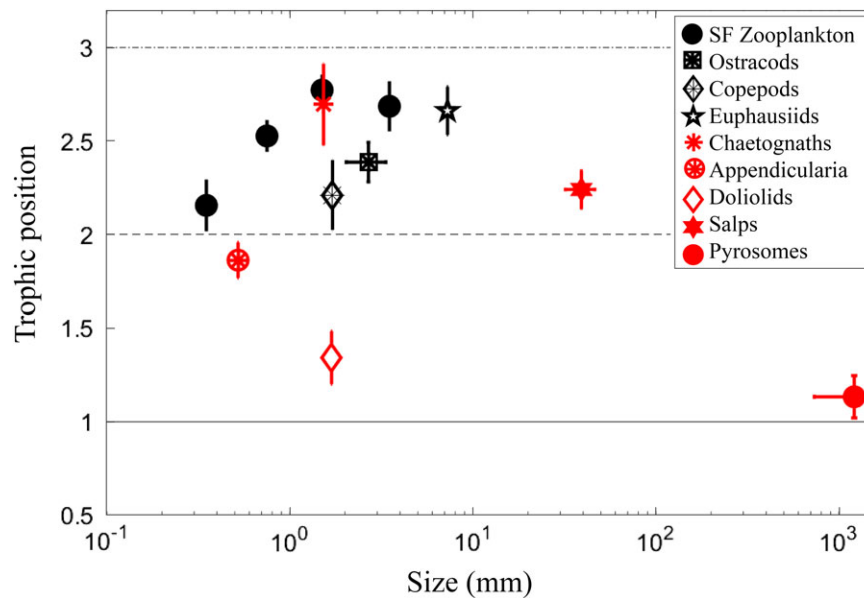
Fig. 6. TP vs. size for bulk mesozooplankton (SF zooplankton = size-fractionated community), and broad taxonomic groups. Markers represent individual zooplankton groups, with gelatinous zooplankton (chaetognaths and pelagic tunicates) plotted in red and the rest of the community in black. Error bars are SE (SF zooplankton $n = 10$, ostracods $n = 15$, copepods $n = 5$, euphausiids $n = 12$, chaetognaths $n = 10$, appendicularia $n = 16$, doliolids $n = 8$, salps $n = 7$, and pyrosomes $n = 5$).

(Fig. 4). Microzooplankton grazing in the upper 40 m was equivalent to 601 ± 61 mg C m^{-2} d^{-1} (Landry et al. 2016*b*), supporting 180 ± 18 mg C m^{-2} d^{-1} of protistan grazers (TP = 2) assuming a gross-growth efficiency of 0.3 (Straile 1997), and 54 ± 5 C m^{-2} d^{-1} secondary consumers (TP = 3). This would be equivalent to 15% of the mesozooplankton phytoplankton consumption, which is an upper-bound as most of the grazing in the upper 40 m occurred in the shallow ML. However, this does not preclude much greater contributions of protistan production in shallower waters, as this process would result in similar isotopic values as the herbivorous pathways, and the small size of phytoplankton requires an intermediate grazer of a size large enough to be consumed by mesozooplankton. Our pigment-derived estimates suggest substantial consumption of phytoplankton by both microzooplankton and mesozooplankton (Décima et al. 2016; Landry et al. 2016*b*), as well as pelagic tunicates, which together add up to ~ 50% of Chl *a* standing stock removed per day (Table 3, Landry et al. 2016*b*). The related pathway of zooplankton feeding on aggregates (Goldthwait et al. 2005; Stukel et al. 2014) containing Chl *a*-degradation products (phaeopigments; Fig. 2b) could also account for some of the measured grazing. Marine snow is hypothesized to be an important source of food for zooplankton (Goldthwait et al. 2004), and the high water-column concentrations of phaeopigments at the base of the euphotic zone suggest that this is an important process in this area (Fig. 2b).

Our combined stable isotope and grazing results suggest different trophic pathways in the water column, with most of the integrated primary production (~ 77%) occurring in the upper 20 m and roughly half of this surface production (47% $\pm$ 34%, mean $\pm$ SE) consumed directly by mesozooplankton (excluding pyrosomes), supporting a multistep food web within the zooplankton (Fig. 7). Waters directly beneath the ML (20–40 m) supported ~ 20% of total PP, and 31% $\pm$ 16% (mean $\pm$ SE) of this subsurface production was consumed by *Pyrostremma spinosum*. Despite a pyrosome standing stock 30 times less than that of mesozooplankton on a dry weight (DW) basis (0.2 $\pm$ 0.1 and 6.2 $\pm$ 0.5 g DW m^{-2}, respectively), their large biovolume and grazing potential, along with reduced PP below the ML, lead to a large impact of pyrosomes on the deeper phytoplankton assemblage not exploited by other mesozooplankton consumers (Fig. 7).

The ecological role of *Pyrostremma spinosum* in the ETP

Our results support the possibility of a unique role for these *pyrosomes* in the ETP, consuming large quantities of phytoplankton below the ML and potentially altering the export of particles to depth. For grazing rate estimates, the gut clearance rate used (0.699 h^{-1}) has considerable uncertainty. We used this value because it was experimentally determined under similar water temperatures (12–15°C; Perissinotto et al. 2007) to our sub-ML thermocline. The rate would presumably be higher for the ML temperature of ~ 27°C (closer to 0.75 h^{-1}; Drits et al. 1992). However, these GCR estimates come from experiments with *P. atlanticum*, a species of much smaller size and firmer consistency than *Pyrostremma spinosum* (Van Soest 1998), and therefore could be different. Regardless of the uncertainty, the high concentrations of ingested pigment in
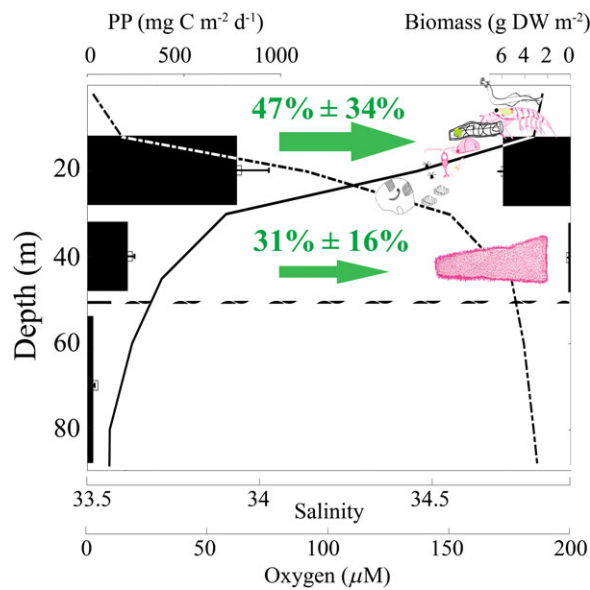
Fig. 7. Schematic of the partitioning of grazing on phytoplankton primary production through the water column, the food-chain within the integrated zooplankton community, and the standing stocks of both *Pyrostremma spinosum* (0.2 ± 0.1 g DW m⁻²) and mesozooplankton (6.2 ± 0.5 g DW m⁻²). PP was integrated for three depth strata (0–20, 21–40, or 41–100 m). Percentages (± SE) denote consumption from each depth strata, where the mesozooplankton community is assumed to graze ML production, while pyrosomes graze on production in the underlying (21–40 m) layer. Dashed-dotted profile denotes salinity, and black profile indicates mean oxygen concentration. Dashed line denotes the average depth of the euphotic zone.

Pyrostremma spinosum zooids still indicate an important grazing role for this pyrosome (Table 2).

The high ratio of (Chl *a* + phaeo) : PE (median = 240 : 1 g : g) in *pyrosoma* zooids indicates that they do not efficiently capture *Synechococcus*. For comparison, where pyrosomes were collected, the ratio of Chl *a* + phaeo : PE in the water column at 20–40 m depth was ~ 5 : 1. The average ratio of PE in > 20-μm aggregates to total water-column PE was closer to 1 : 7, suggesting that aggregate-associated *Synechococcus* ingestion would be sufficient to explain zooid PE concentrations. Individual colonies consumed an average of 0.8 mg Chl *a* h⁻¹ (range 0.2–2.1 mg Chl *a* h⁻¹). We can estimate the volume filtered by a colony using average Chl *a* concentrations in the 20–40 m depth range (0.27 ± 0.08 mg Chl *a* m⁻³) and measured pigment ingestion. Colonies of 1.2–3.7 liters in volume had clearance rates of 3 ± 1 m³ colony⁻¹ h⁻¹ (mean ± SE). For comparison, the average clearance rates of ~ 55-mm colonies of *P. atlanticum* was determined to be 5.5 L colony⁻¹ h⁻¹ (Drits et al. 1992), which results in very different clearance rates per zooid. The 55-mm *P. atlanticum* had ~ 1412 zooids per colony (Andersen and Sardou 1994) and *Pyrostremma spinosum* in our study had 2000–20,000 zooids per colony while reaching much larger sizes (Table 1), which translates to a ~ 2 order of magnitude increase in zooid clearance rate, from 3.5 mL zooid⁻¹ h⁻¹ (*P. atlanticum*) to 450 mL zooid⁻¹ h⁻¹ (*Pyrostremma spinosum*).

Unfortunately, we do not have zooid size estimates for either of these species to evaluate this scaling effect. However, if we scale these rates with colony length, using the zooid/length relationships above, we estimate that a 1 m-long *P. atlanticum* would filter ~ 1.6 m⁻³ colony⁻¹ h⁻¹, which is in the range of the estimates for *pyrosomes* in this study.

Our identification was based on the characteristics described by Van Soest (1998), and in that study, *Pyrostremma spinosum* is not indicated to inhabit the ETP, and we have found no additional references of this species in the area. However, in the same study, Van Soest (1998) summarizes the bioregions in which each species of pyrosoma has been observed. While no records of *Pyrostremma spinosum* were listed for the ETP, observations were listed for the two contiguous bioregions (not separated by land or major oceanographic features), the equatorial and southwest Pacific, and a congeneric species (*Pyrostremma agassizi*) have been observed within the ETP. It is likely that the lack of studies in this area have contributed to our sparse understanding of its distribution and ecology. The only other study to document the habitat for *Pyrosoma spinosum* was done in the Arabian Sea (Gauns et al. 2015). In this area, *Pyrosoma spinosum* was found under conditions of high macronutrient concentrations, modest Chl *a*, dominance of *Synechococcus* in the upper 40 m, and overlying a well-developed shallow oxygen minimum zone, all of which are very similar to the characteristics of our study area (Buchwald et al. 2015; Selph et al. 2016), and suggest these as typical habitat characteristics for *Pyrosoma spinosum*.

It is unclear if *P. spinosum* functions mainly as a "flux-feeder," a suspension-feeding grazer of phytoplankton and protists (Table 2), or some combination of the two. The higher ratio of phaeo : Chl *a* in the depth range where it feeds (Fig. 2a,b) suggests that these *pyrosomes* may consume some fecal material produced by other mesozooplankton. The δ^{13}C and δ^{15}N of *Pyrostremma spinosum* (1–3.5‰ and ~ 5‰ lower than for other mesozooplankton), however, would suggest this process is minor, as larger isotope depletion of feces with respect to body tissues would be required (Checkley and Entzeroth 1985) yet imply higher TDFs that would lead to unrealistically low TPs. It is more likely, from the stable isotope perspective, that the bulk zooplankton is consuming high levels of fecal material. While the relative contributions of fresh phytoplankton, fecal pellets, and other detritus in the diet of *Pyrostremma spinosum* cannot be determined with certainty, the isotopic composition of exported material (at a depth of 90 m) more closely resembles *Pyrostremma spinosum* than either POM or zooplankton from the ML. The mismatch between the isotopic compositions of both ML POM (where most primary productivity occurs) and suspended deep POM from sinking material suggests a transformation mediated by zooplankton (Stukel et al. 2011; Turner 2015) or microbial reprocessing (Legendre and Lefevre 1995). Calculations of the total particulate carbon egested by pyrosomes, 18.9 ± 18.3 (Table 6), are equivalent to about 30% of the regional mean

Table 6. Potential contribution of *Pyrostremma spinosum* and the mesozooplankton size-fractionated community to export flux, assuming egestion = 0.3 consumption, and using C : Chl from the assumed feeding depths of each group, from Taylor et al. (2016).

Cycle	POC flux (90 m) (mg C m^{-2} d^{-1})	*P. spinosum* colony fecal production (mg C m^{-2} d^{-1})	Zooplankton size-fractionated community fecal production (mg C m^{-2} d^{-1})	% POC export *P. spinosum* fecal production	% POC export zooplankton fecal production
2	63.9 ± 18.0	8.0 ± 5.8*	54.6 ± 8.1	12.5 ± 9.1*	85.5 ± 12.7
3	67.3 ± 4.8	1.6 ± 1.2*	225.9 ± 93.3	2.4 ± 1.8*	335.6 ± 138.7
4	50.3 ± 6.0	42.6 ± 16.3	91.4 ± 35.0	84.6 ± 32.4	181.7 ± 69.5
5	72.4 ± 6.0	23.5 ± 8.8	315.5 ± 55.0	32.4 ± 12.1	435.5 ± 75.9
Mean[†]	63.5 ± 9.5	18.9 ± 18.3	171.9 ± 120.8	29.8 ± 28.8	259.6 ± 156.1

*These estimates were based on recorded volumes of collected pyrosomes (Table 1) and estimated mean grazing rate per milliliter of colony, assuming 4.5 d (cycle duration).

[†]Mean cruise estimates were made using measured grazing of pyrosomes when possible, and including the estimates for Cycle 2 and Cycle 3, normalized to 18 sampling days—the length of the four cycles considered here (there is no sediment trap data for the transect stations, hence that estimate was not included here).

POC collected in sediment traps at 90 m, while the mesozooplankton community produce feces calculated to be ~ 260% of sinking POC (Stukel et al. 2016). The excess of grazing over export by the combined mesozooplankton/*Pyrostremma spinosum* community indicates that most egested material is substantially reworked before sinking (Stukel et al. 2016) and is supported by the change in phaeo : Chl *a* ratio with depth.

The distinct isotopic values of *Pyrostremma spinosum*, signaling a specific depth of feeding (20–40 m, Figs. 4, 7), begs the question of why these organisms feed at a different depth than the rest of the community. Perhaps their nutritional requirements are different, as trace metal ratios were depth specific, with higher Fe : S (but lower Zn : S and Ni : S) in the subsurface chlorophyll maximum compared to the surface (Baines et al. 2016). Particle aggregation at the bottom of the ML may also lead to higher concentrations of large particles, satisfying the nutritional requirements of *Pyrostremma spinosum*, while limiting other zooplankton due to low Zn and Ni (Baines et al. 2016). This could also explain why the isotopic values of exported POC and *Pyrostremma spinosum* are so similar, as both would be fueled by larger particles forming or concentrating below the ML. Finally, these organisms may prefer the cooler temperatures, reduced turbulence levels beneath the ML, or be potentially better equipped to survive the low oxygen concentrations. Regardless, by directly consuming larger particles in a portion of the euphotic zone not heavily exploited by the rest of the mesozooplankton community, *Pyrostremma spinosum* represents a distinct pathway of material and energy transfer to higher trophic levels in the ETP.

References

Alldredge, A. L. 1972. Abandoned larvacean houses: Unique food source in the pelagic environment. Science **177**: 885–887. doi:10.1126/science.177.4052.885

Alldredge, A. L., and L. P. Madin. 1982. Pelagic tunicates: Unique herbivores in the marine plankton. Bioscience **32**: 655–663. doi:10.2307/1308815

Andersen, V. 1998. Salp and pyrosomid blooms and their importance in biogeochemical cycles, p. 125–137. *In* Q. Bone [ed.], The biology of pelagic tunicates. Oxford Univ. Press.

Andersen, V., J. Sardou, and P. Nival. 1992. The diel migrations and vertical distributions of zooplankton and micronekton in the northwestern Mediterranean Sea. 2. Siphonophores, hydromedusae and pyrosomids. J. Plankton Res. **14**: 1155–1169. doi:10.1093/plankt/14.8.1155

Andersen, V., and J. Sardou. 1994. *Pyrosoma atlanticum* (Tunicata, Thaliacea): Diel migration and vertical distribution as a function of colony size. J. Plankton Res. **16**: 337–349. doi:10.1093/plankt/16.4.337

Baines, S. B., X. Chen, S. Vogt, N. S. Fisher, B. S. Twining, and M. R. Landry. 2016. Microplankton trace element contents: Implications for mineral limitation of mesozooplankton in an HNLC area. J. Plankton Res. **38**: 256–270. doi:10.1093/plankt/fbv109

Ballance, L. T., R. L. Pitman, and P. C. Fiedler. 2006. Oceanographic influences on seabirds and cetaceans of the eastern tropical Pacific: A review. Prog. Oceanogr. **69**: 360–390. doi:10.1016/j.pocean.2006.03.013

Bone, Q. 1998. The biology of pelagic tunicates. Oxford Univ. Press.

Brodeur, R. D., and others. 2018. An unusual gelatinous event in the NE Pacific: The great pyrosome bloom of 2017. North Pacific Marine Science Organization. doi:10.1007/s10803-018-3619-5

Buchwald, C., A. E. Santoro, R. H. R. Stanley, and K. L. Casciotti. 2015. Nitrogen cycling in the secondary nitrite maximum of the eastern tropical North Pacific off Costa Rica. Global Biogeochem. Cycle **29**: 2061–2081. doi:10.1002/2015gb005187

Calbet, A., and M. R. Landry. 1999. Mesozooplankton influences on the microbial food web: Direct and indirect trophic interactions in the oligotrophic open ocean. Limnol. Oceanogr. **44**: 1370–1380. doi:10.4319/lo.1999.44.6.1370

Checkley, D. M., and L. C. Entzeroth. 1985. Elemental and isotopic fractionation of carbon and nitrogen by marine, planktonic copepods and implications to the marine nitrogen cycle. J. Plankton Res. **7**: 553–568. doi:10.1093/plankt/7.4.553

Chouvelon, T., J. Spitz, F. Caurant, P. Mendez-Fernandez, A. Chappuis, F. Laugier, E. Le Goff, and P. Bustamante. 2012. Revisiting the use of delta N-15 in meso-scale studies of marine food webs by considering spatio-temporal variations in stable isotopic signatures—the case of an open ecosystem: The Bay of Biscay (north-East Atlantic). Prog. Oceanogr. **101**: 92–105. doi:10.1016/j.pocean.2012.01.004

Conover, R. J. 1966. Factors affecting assimilation of organic matter by zooplankton and question of superfluos feeding. Limnol. Oceanogr. **11**: 346–354. doi:10.4319/lo.1966.11.3.0346.

Décima, M., M. R. Landry, and B. N. Popp. 2013. Environmental perturbation effects on baseline $\delta^{15}N$ values and zooplankton trophic flexibility in the southern California current ecosystem. Limnol. Oceanogr. **58**: 624–634. doi:10.4319/lo.2013.58.2.0624

Décima, M., M. R. Landry, M. R. Stukel, L. Lopez-Lopez, and J. W. Krause. 2016. Mesozooplankton biomass and grazing in the Costa Rica dome: Amplifying variability through the plankton food web. J. Plankton Res. **38**: 317–330. doi:10.1093/plankt/fbv091

Décima, M., M. R. Landry, C. J. Bradley, and M. L. Fogel. 2017. Alanine $\delta^{15}N$ trophic fractionation in heterotrophic protists. Limnol. Oceanogr. **62**: 2308–2322. doi:10.1002/lno.10567.

Deibel, D. 1998. The abundance, distribution, and ecological impact of doliolids, p. 171–185. *In* Q. Bone [ed.], The biology of pelagic tunicates. Oxford Univ. Press.

Deibel, D., J. F. Cavaletto, M. Riehl, and W. S. Gardner. 1992. Lipid and lipid class content of the pelagic tunicate *Oikopleura vanhoeffeni*. Mar. Ecol. Prog. Ser. **88**: 297–302. doi:10.3354/meps088297

Dore, J. E., J. Brum, L. M. Tupas, and D. M. Karl. 2002. Seasonal and interannual variability in sources of nitrogen supporting export in the oligotrophic subtropical North Pacific Ocean. Limnol. Oceanogr. **47**: 1595–1607. doi:10.4319/lo.2002.47.6.1595

Drits, A. V., E. G. Arashkevich, and T. N. Semenova. 1992. *Pyrosoma atlanticum* (Tunicata, Thaliacea): Grazing impact on phytoplankton standing stock and role in organic carbon flux. J. Plankton Res. **14**: 799–809. doi:10.1093/plankt/14.6.799

Fenaux, R., Q. Bone, and D. Deibel. 1998. Appendicularian distribution and zoogeography, p. 251–263. *In* Q. Bone [ed.], The biology of pelagic tunicates. Oxford Univ. Press.

Fessenden, L., and T. J. Cowles. 1994. Copepod predation on phagotrophic ciliates in Oregon coastal waters. Mar. Ecol. Prog. Ser. **107**: 103–111. doi:10.3354/meps107103

Fiedler, P. C. 2002. The annual cycle and biological effects of the Costa Rica dome. Deep-Sea Res. Part I **49**: 321–338. doi:10.1016/S0967-0637(01)00057-7

Gauns, M., S. Mochemadkar, A. Pratihary, R. Roy, and S. W. A. Naqvi. 2015. Biogeochemistry and ecology of *Pyrosoma spinosum* from the central Arabian Sea. Zool. Stud. **54**: 17. doi:10.1186/s40555-014-0075-6

Goldthwait, S., J. Yen, J. Brown, and A. Alldredge. 2004. Quantification of marine snow fragmentation by swimming euphausiids. Limnol. Oceanogr. **49**: 940–952. doi:10.4319/lo.2004.49.4.0940

Goldthwait, S. A., C. A. Carlson, G. K. Henderson, and A. L. Alldredge. 2005. Effects of physical fragmentation on remineralization of marine snow. Mar. Ecol. Prog. Ser. **305**: 59–65. doi:10.3354/meps305059

Gorsky, G., and R. Fenaux. 1998. The role of Appendicularia in marine food webs, p. 161–169. *In* Q. Bone [ed.], The biology of pelagic tunicates. Oxford Univ. Press.

Griffin, D. J. G., and J. C. Yaldwyn. 1970. Giant colonies of pelagic tunicates (Pyrosoma spinosum) from SE Australia and New Zealand. Nature **226**: 464. doi:10.1038/226464a0

Gutiérrez-Rodríguez, A., M. Décima, B. N. Popp, and M. R. Landry. 2014. Isotopic invisibility of protozoan trophic steps in marine food webs. Limnol. Oceanogr. **59**: 1590–1598. doi:10.4319/lo.2014.59.5.1590

Henschke, N., J. D. Everett, A. J. Richardson, and I. M. Suthers. 2016. Rethinking the role of salps in the ocean. Trends Ecol. Evol. **31**: 720–733. doi:10.1016/j.tree.2016.06.007

Hereu, C. M., B. E. Lavaniegos, and R. Goericke. 2010. Grazing impact of salp (Tunicata, Thaliacea) assemblages in the eastern tropical North Pacific. J. Plankton Res. **32**: 785–804. doi:10.1093/plankt/fbq005

Kuo, C. Y., T. Y. Fan, H. H. Li, C. W. Lin, L. L. Liu, and F. W. Kuo. 2015. An unusual bloom of the tunicate, *Pyrosoma atlanticum*, in southern Taiwan. Bull. Mar. Sci. **91**: 363–364. doi:10.5343/bms.2014.1090

Landry, M. R., A. De Verneil, J. I. Goes, and J. W. Moffett. 2016a. Plankton dynamics and biogeochemical fluxes in the Costa Rica dome: Introduction to the CRD flux and zinc experiments. J. Plankton Res. **38**: 167–182. doi:10.1093/plankt/fbv103

Landry, M. R., K. E. Selph, M. Décima, A. Gutiérrez-Rodríguez, M. R. Stukel, A. G. Taylor, and A. L. Pasulka. 2016b. Phytoplankton production and grazing balances in the Costa Rica dome. J. Plankton Res. **38**: 366–379. doi:10.1093/plankt/fbv089

Landry, M. R., and M. Décima. 2017. Protistan microzooplankton and the trophic position of tuna: Quantifying the trophic link between micro- and mesozooplankton in marine food webs. ICES J. Mar. Sci. **74**: 1885–1892. doi:10.1093/icesjms/fsx006

Lebrato, M., and D. O. B. Jones. 2009. Mass deposition event of *Pyrosoma atlanticum* carcasses off Ivory Coast (West Africa). Limnol. Oceanogr. **54**: 1197–1209. doi:10.4319/lo.2009.54.4.1197

Lee, R. F., W. Hagen, and G. Kattner. 2006. Lipid storage in marine zooplankton. Mar. Ecol. Prog. Ser. **307**: 273–306. doi:10.3354/meps307273

Legendre, L., and J. Lefevre. 1995. Microbial food-webs and the export of biogenic carbon in oceans. Aquat. Microb. Ecol. **9**: 69–77. doi:10.3354/ame009069

Li, W. K. W., D. V. Subba Rao, W. G. Harrison, J. C. Smith, J. J. Cullen, B. Irwin, and T. Platt. 1983. Autotrophic picoplankton in the tropical ocean. Science **219**: 292–295. doi:10.1126/science.219.4582.292

Liao, Z. H., H. Y. Hsieh, and W. T. Lo. 2013. Influence of monsoon-driven hydrographic features on thaliacean distribution in waters around Taiwan, western North Pacific Ocean. Zool. Stud. **52**: 1–14. doi:10.1186/1810-522x-52-49

Liu, H. B., M. J. Dagg, and S. Strom. 2005. Grazing by the calanoid copepod *Neocalanus cristatus* on the microbial food web in the coastal Gulf of Alaska. J. Plankton Res. **27**: 647–662. doi:10.1093/plankt/fbi039

Logan, J. M., T. D. Jardine, T. J. Miller, S. E. Bunn, R. A. Cunjak, and M. E. Lutcavage. 2008. Lipid corrections in carbon and nitrogen stable isotope analyses: Comparison of chemical extraction and modelling methods. J. Anim. Ecol. **77**: 838–846. doi:10.1111/j.1365-2656.2008.01394.x

Lombard, F., and T. Kiørboe. 2010. Marine snow originating from appendicularian houses: Age-dependent settling characteristics. Deep-Sea Res. Part I **57**: 1304–1313. doi:10.1016/j.dsr.2010.06.008

Madin, L. P. 1982. Production, composition and sedimentation of salp fecal pellets in oceanic waters. Mar. Biol. **67**: 39–45. doi:10.1007/bf00397092

Madin, L. P., C. M. Cetta, and V. L. Mcalister. 1981. Elemental and biochemical-composition of Salps (Tunicata, Thaliacea). Mar. Biol. **63**: 217–226. doi:10.1007/BF00395990

Madin, L. P., and P. Kremer. 1995. Determination of the filter feeding rates of salps (Tunicata, Thaliacea). ICES J. Mar. Sci. **52**: 583–595. doi:10.1016/1054-3139(95)80073-5.

Madin, L. P., P. Kremer, P. H. Wiebe, J. E. Purcell, E. H. Horgan, and D. A. Nemazie. 2006. Periodic swarms of the salp *Salpa aspera* in the slope water off the NE United States: Biovolume, vertical migration, grazing, and vertical flux. Deep-Sea Res. Part I **53**: 804–819. doi:10.1016/j.dsr.2005.12.018

Michaels, A. F., and M. W. Silver. 1988. Primary production, sinking fluxes and the microbial food web. Deep-Sea Res. Part I **35**: 473–490. doi:10.1016/0198-0149(88)90126-4

Mintenbeck, K., T. Brey, U. Jacob, R. Knust, and U. Struck. 2008. How to account for the lipid effect on carbon stable-isotope ratio (delta C-13): Sample treatment effects and model bias. J. Fish Biol. **72**: 815–830. doi:10.1111/j.1095-8649.2007.01754.x

Nelson, M. M., C. F. Phleger, B. D. Mooney, and P. D. Nichols. 2000. Lipids of gelatinous Antarctic zooplankton: Cnidaria and Ctenophora. Lipids **35**: 551–559. doi:10.1007/s11745-000-555-5

Perissinotto, R., P. Mayzaud, P. D. Nichols, and J. P. Labat. 2007. Grazing by *Pyrosoma atlanticum* (Tunicata, Thaliacea) in the South Indian Ocean. Mar. Ecol. Prog. Ser. **330**: 1–11. doi:10.3354/meps330001

Post, D. M. 2002. Using stable isotopes to estimate trophic position: Models, methods, and assumptions. Ecology **83**: 703–718. doi:10.1890/0012-9658.

Post, D. M., C. A. Layman, D. A. Arrington, G. Takimoto, J. Quattrochi, and C. G. Montana. 2007. Getting to the fat of the matter: Models, methods and assumptions for dealing with lipids in stable isotope analyses. Oecologia **152**: 179–189. doi:10.1007/s00442-006-0630-x

Rau, G. H., M. D. Ohman, and A. Pierrot-Bults. 2003. Linking nitrogen dynamics to climate variability off Central California: A 51 year record based on $^{15}N/^{14}N$ in CalCOFI zooplankton. Deep-Sea Res. Part II **50**: 2431–2447. doi:10.1016/S0967-0645(03)00128-0

Ricca, M. A., A. K. Miles, R. G. Anthony, X. Deng, and S. S. O. Hung. 2007. Effect-of lipid extraction on analyses of stable carbon and stable nitrogen isotopes in coastal organisms of the Aleutian archipelago. Can. J. Zool.-Rev. Can. Zool. **85**: 40–48. doi:10.1139/z06-187

Roman, M. R., and A. L. Gauzens. 1997. Copepod grazing in the equatorial Pacific. Limnol. Oceanogr. **42**: 623–634. doi:10.4319/lo.1997.42.4.0623

Sakuma, K. M., J. C. Field, N. J. Mantua, S. Ralston, B. B. Marinovic, and C. N. Carrion. 2016. Anomalous epipelagic micronekton assemblage patterns in the neritic waters of the California current in spring 2015 during a period of extreme ocean conditions. Calif. Coop. Ocean. Fish. Invest. Rep. **57**: 163–183.

Scheinberg, R. D., and M. R. Landry. 2005. Clearance rates and efficiencies of Oikopleura fusiformis on the natural prey assemblage of a subtropical coastal ecosystem, p. 214–230. *In* G. Gorsky, D. Deibel, and M. Youngbluth [eds.], Response of marine ecosystems to global change: Ecological impact of Appendicularians. Gordon & Breach Scientific Publishers.

Scheinberg, R. D., M. R. Landry, and A. Calbet. 2005. Grazing of two common appendicularians on the natural prey assemblage of a tropical coastal ecosystem. Mar. Ecol. Prog. Ser. **294**: 201–212. doi:10.3354/meps294201

Selph, K. E., M. R. Landry, A. G. Taylor, A. Gutierrez-Rodriguez, M. R. Stukel, J. Wokuluk, and A. Pasulka. 2016. Phytoplankton production and taxon-specific growth rates in the Costa Rica dome. J. Plankton Res. **38**: 199–215. doi:10.1093/plankt/fbv063

Smith, K. L., and others. 2014. Large salp bloom export from the upper ocean and benthic community response in the abyssal Northeast Pacific: Day to week resolution. Limnol. Oceanogr. **59**: 745–757. DOI:10.4319/lo.2014.59.3.0745

Stoecker, D. K., and J. M. Capuzzo. 1990. Predation on protozoa: Its importance to zooplankton. J. Plankton Res. **12**: 891–908. doi:10.1093/plankt/12.5.891

Stone, J. P., and D. K. Steinberg. 2016. Salp contributions to vertical carbon flux in the Sargasso Sea. Deep-Sea Res. Part I **113**: 90–100. https://doi.org/10.1016/j.dsr.2016.04.007.

Straile, D. 1997. Gross growth efficiencies of protozoan and metazoan zooplankton and their dependence on food concentration, predator-prey weight ratio, and taxonomic group. Limnol. Oceanogr. **42**: 1375–1385. doi:10.4319/lo.1997.42.6.1375

Strickland, J. D. H., and T. R. Parsons. 1972. A practical handbook of seawater analysis. Fisheries Research Board of Canada. doi:10.1016/S0022-3476(72)80550-X

Stukel, M. R., M. R. Landry, C. R. Benitez-Nelson, and R. Goericke. 2011. Trophic cycling and carbon export relationships in the California current ecosystem. Limnol. Oceanogr. **56**: 1866–1878. doi:10.4319/lo.2111.56.5.1866

Stukel, M. R., M. Décima, K. E. Selph, D. A. A. Taniguchi, and M. R. Landry. 2013. The role of Synechococcus in vertical flux in the Costa Rica upwelling dome. Prog. Oceanogr. **112**: 49–59. doi:10.1016/j.pocean.2013.04.003

Stukel, M. R., K. A. Smith, M. Décima, and L. Hmelo. 2014. Detritus in the marine environment, p. 49–76. *In* P. F. Kemp [ed.], Eco-DAS IX Symposium Proceedings. Association for the Sciences of Limnology and Oceanography.

Stukel, M. R., C. R. Benitez-Nelson, M. Décima, A. G. Taylor, C. Buchwald, and M. R. Landry. 2016. The biological pump in the Costa Rica dome: An open-ocean upwelling system with high new production and low export. J. Plankton Res. **38**: 348–365. doi:10.1093/plankt/fbv097

Sutherland, K. R., L. P. Madin, and R. Stocker. 2010. Filtration of submicrometer particles by pelagic tunicates. Proc. Natl. Acad. Sci. USA **107**: 15129–15134. doi:10.1073/pnas.1003599107

Takahashi, K., T. Ichikawa, C. Fukugama, M. Yamane, S. Kakehi, Y. Okazaki, H. Kubota, and K. Furuya. 2015. In situ observations of a doliolid bloom in a warm water filament using a video plankton recorder: Bloom development, fate, and effect on biogeochemical cycles and planktonic food webs. Limnol. Oceanogr. **60**: 1763–1780. doi:10.1002/lno.10133

Taylor, A. G., M. R. Landry, A. Freibott, K. E. Selph, and A. Gutierrez-Rodriguez. 2016. Patterns of microbial community biomass, composition and HPLC diagnostic pigments in the Costa Rica upwelling dome. J. Plankton Res. **38**: 183–198. doi:10.1093/plankt/fbv086

Tobena, M., and A. Escanez. 2013. Registration of an aggregation of *Pyrosoma atlanticum* Peron 1804 (Thaliacea, Tunicata) in waters around the island of El Hierro, Canary Islands. Rev. Acad. Canaria Ciencias **25**: 35–43.

Turner, J. T. 2015. Zooplankton fecal pellets, marine snow, phytodetritus and the ocean's biological pump. Prog. Oceanogr. **130**: 205–248. doi:10.1016/j.pocean.2014.08.005

Ute, J., M. Katja, B. Thomas, K. Rainer, and B. Kerstin. 2005. Stable isotope food web studies: A case for standardized sample treatment. Mar. Ecol. Prog. Ser. **287**: 251–253.

Vander Zanden, M. J., and J. B. Rasmussen. 2001. Variation in $\delta^{15}N$ and $\delta^{13}C$ trophic fractionation: Implications for aquatic food web studies. Limnol. Oceanogr. **46**: 2061–2066. doi:10.4319/lo.2001.46.8.2061

Van Soest, R. W. M. 1981. A monograph of the order Pyrosomatida (Tunicata, Thaliacea). J. Plankton Res. **3**: 603–631. doi:10.1093/plankt/3.4.603

Van Soest, R. W. M. 1998. The cladistic biogeography of salps and pyrosomas, p. 231–249. *In* Q. Bone [ed.], The biology of pelagic tunicates. Oxford Univ. Press.

Williams, R. L., S. Wakeham, R. Mckinney, and K. F. Wishner. 2014. Trophic ecology and vertical patterns of carbon and nitrogen stable isotopes in zooplankton from oxygen minimum zone regions. Deep-Sea Res. Part I **90**: 36–47. doi:10.1016/j.dsr.2014.04.008

Wyman, M. 1992. An in vivo method for the estimation of phycoerythrin concentrations in marine cyanobacteria (*Synechococcus* spp.). Limnol. Oceanogr. **37**: 1300–1306. doi:10.4319/lo.1992.37.6.1300

Zhang, X., H. G. Dam, J. R. White, and M. R. Roman. 1995. Latitudinal variations in mesozooplankton grazing and metabolism in the central tropical Pacific during the US JGOFS EqPac study. Deep-Sea Res. II **42**: 695–714. doi:10.1016/0967-0645(95)00032-L

Zubkov, M. V., and A. Lopez-Urrutia. 2003. Effect of appendicularians and copepods on bacterioplankton composition and growth in the English Channel. Aquat. Microb. Ecol. **32**: 39–46. doi:10.3354/ame032039

Conflict of Interest

None declared.